Session A1 : Silencieux et tuyaux flexibles – Mufflers and flexible ducts

Sound attenuation in absorbing ducts by wall permeability and structural interaction effects

Utilisation de la perméabilité des parois et des effets de couplage avec la structure pour l'absorption acoustique des conduits

L'absorption du son par des tubes poreux à parois perméables, ainsi que par des conduits à parois flexibles avec revêtement acoustique intérieur est étudiée. Il est démontré que les premiers peuvent effectivement se comporter comme des silencieux sur une grande plage de fréquences. Quant aux seconds, ils peuvent fournir une très forte atténuation dans des bandes étroites de fréquence, et ceci par effet de résonance de structure avec amortissement,. Les mécanismes physiques, ainsi que des applications pratiques de ces systèmes sont exposés.

A. Cummings,
Department of Engineering,
University of Hull,
Hull HU6 7RX,
UK

Porous sound absorbents are widely used in duct attenuators, usually in the form of wall linings or as baffles that are placed parallel to the airflow. In these configurations, they can provide high attenuation at mid to high frequencies, but their acoustic performance falls off dramatically at low frequencies. This is partly because of the relatively low acoustic particle velocity in the material, caused by the fact that the lining thickess is only a small fraction of a wavelength.

There are several ways of increasing the low frequency absorption of sound by porous media. Two that have received relatively little attention are: first, ducts made with porous walls but no impervious external cladding, and secondly, ducts with elastic outer walls and an inner lining of porous material placed immediately adjacent to the outer wall.

Porous tubes, usually consisting of woven cotton reinforced by a steel wire spiral, are currently widely employed in automotive engine intake systems, between the air inlet and the air filter. Intake noise, propagating upstream, creates acoustic particle motion through the porous walls of the tube. Since there is no impervious wall to prevent radial particle motion on the exterior surface of the tube, the radial particle velocity is restricted only by the normal impedance of the tube wall. Clearly there is radiation to the exterior as well as axially within the porous tube, but high net attenuation of the incident sound power is possible, and it does not appear to fall off significantly at low frequencies. Cummings and Kirby [1] have presented an analysis of sound propagation in, and radiation from, tubes with permeable walls and have compared predicted and measured data.

Sheet metal ducts with internal linings are widely used in air-moving ducts and, indeed, the aforementioned baffle type silencers usually fall into this category. In commercial types of silencer, any improvement in sound attenuation produced by the juxtaposition of absorbent and flexible wall – over and above that expected from a rigid-walled silencer – is not usually noticeable. However, if special efforts are made to ensure that the air-gap between absorbent and duct wall is very small, it is possible to achieve very high attenuation in a marrow frequency band around the fundamental structural transverse resonant frequency of the duct walls. Astley, Cummings and Sormaz [2] noted this effect, and obtained good agreement between numerically predicted and measured data on a rectangular section duct with three rigid walls and one flexible wall, against which was placed an internal acoustic liner.

They noted an increase in attenuation at the fundamental wall resonant frequency of about a factor of ten, as compared to the equivalent rigid-walled duct. Kirby and Cummings [3] presented a finite element scheme for the prediction of sound transmission in rectangular section ducts with four flexible walls, internally lined on all walls. This too forecasts a substantial attenuation peak at the lowest transverse wall resonant frequency of either rectangular or square section ducts. The attenuation mechanism here is a "gas-pumping" process whereby the vibrating duct wall forces air through the pores of the absorbent at the structural resonant frequency, causing large acoustic losses via viscous dissipation. A similar mechanism has been reported by Cummings, Rice and Wilson [4] in the case of a rectangular plate radiating sound into a nearby porous medium.

Large values of radiation efficiency and consequent panel damping were both predicted and measured. The radiation mechanism in this case was interpreted as acoustic energy loss by near-field absorption in a dissipative medium, this description may also be applied to the case of flexible-walled lined ducts.

In this paper predictive mathematical models for sound absorption, by both tubes with permeable walls and by elastic-walled ducts with internal linings, are briefly described, emphasis being placed on the physical processes involved. Some representative predicted and measured data are shown, and practical applications and implications of the two sound attenuation mechanisms described are outlined.

Tubes with permeable walls

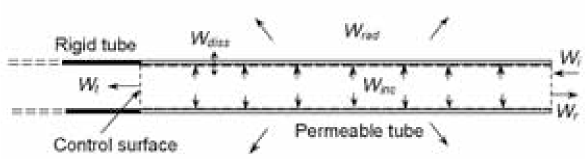

Fig. 1 : A tube with permeable walls

A tube with permeable walls is show in Figure 1; it is assumed to be terminated anechoically by a rigid tube at its left-hand end. Sound power W_i enters the tube from a source at the right-hand end. Sound power W_r may be reflected back toward the source (as, for example, at an impedance discontinuity where a rigid-walled tube meets the permeable-walled tube) and the balance will be transmitted into the permeable tube. Of this, an amount W_t will be transmitted at the far end of the tube and a net amount $W_{inc} = W_i - W_r - W_t$ will be incident on the tube walls. Some of this, W_{diss}, will be dissipated in the tube walls, while a residual amount, W_{rad}, will be radiated to the exterior of the tube. We may define an "internal transmission loss" (not including the radiated or dissipated sound power),

$$TL = 10\mathrm{Log}(W_i / W_t) \qquad (1)$$

A "radiation loss" may also be defined, relating the radiated sound power to the incident power (giving a measure of the "leakage" of sound out through the tube walls),

$$\Delta_{rad} = 10\mathrm{Log}(W_i / W_{rad}) \qquad (2)$$

The predictive model is described in detail by Cummings and Kirby [1] and therefore only some of the salient points will be outlined here. It is assumed that the frequency is low enough so that only the fundamental acoustic mode within the tube propagates. The external radiation load is taken into account, and therefore the normal impedance on the interior wall of the tube will vary along the length of the tube, even if the wall impedance (interior/exterior sound pressure differential ÷ normal particle velocity) is constant. The tube is divided axially into cells, within each of which the wall impedance is assumed constant, so that the sound pressures in the incident and reflected waves may be written

$$p_i(r,x;t) = e^{i\omega t} P_i e^{ik_x x} J_0(k_r r), \qquad (3a)$$

$$p_r(r,x;t) = e^{i\omega t} P_r e^{-ik_x x} J_0(k_r r), \qquad (3b)$$

where P represents sound pressure amplitude, K_x, K_r are axial and radial wavenumbers for the fundamental mode, the radial factor in the sound field is $J_0(K_r r)$ and $J_m(\ \ )$ is a Bessel function. Two adjacent cells are depicted in Figure 2.

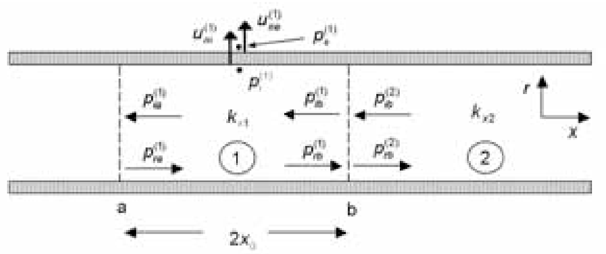

Fig. 2 : Two adjacent cells

Sound pressures and volume velocities are matched at the boundaries between cells (e.g. at "b" in Figure 2), and incident and reflected sound pressures are found for all cells in the tube. The radiation load is found by an iterative procedure. The model was verified by tests on a perforated aluminium tube, and analytical methods were used to predict the wall impedance. Measured and predicted sound fields within the tube were in good agreement, and it transpired that the radiation load was of great importance in determining the internal sound field, especially at the lower frequencies. An example of such a comparison is shown in Figure 3. The tube in this case was rigidly terminated at x = 0. It can be seen that radiation from the tube has a very large effect on the internal sound field, and that predictions and measurements agree very well.

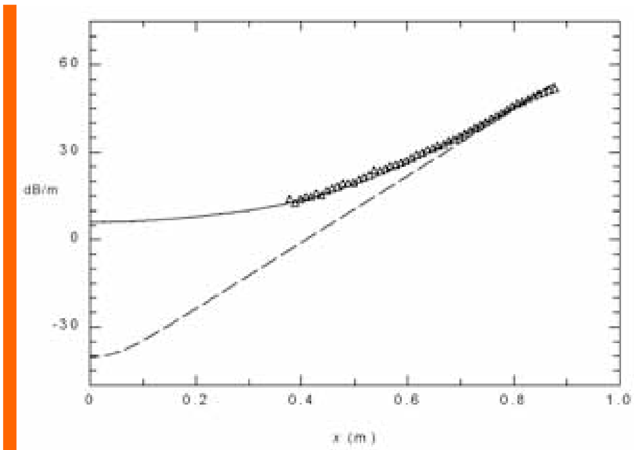

Fig. 3 : Predicted and measured axial sound pressure level distribution in a perforated aluminium tube at 200 Hz: ——, predicted with radiation load; — — —, predicted without radiation load; Δ, measured data.

Of more interest in the present context are typical results on permeable fabric tubes. It proved extremely difficult to measure the wall impedance of these tubes directly (this is a topic ideal for further investigation), and "best fit" wall impedance figures had to be used. Agreement between predicted and measured internal sound fields was generally good, and an example is given in Figure 4, at 1 kHz, again with a rigid termination. The length of the tube was 776mm and its internal diameter was 55mm. The best fit wall impedance value, in rc units, is given in the caption and, as expected, indicates a mass type reactance. Sound power data for this tube are given in Table 1. These are, of course, only relative figures. In the computation, the sound pressure amplitude in the incident wave in the rigid-walled tube remote from the source was put equal to 1 Pa.

Table 1. Sound power components and transmission, radiation losses for the fabric tube.

f (Hz)	W_i (Watt)	W_r (Watt)	W_t (Watt)	W_{rad} (Watt)	W_{diss} (Watt)	TL (dB)	Δ_{rad} (dB)
250	4.12×10^{-2}	1.09×10^{-6}	2.88×10^{-6}	7.68×10^{-4}	4.04×10^{-2}	41.6	17.3
500	1.77×10^{-2}	2.95×10^{-7}	2.88×10^{-6}	3.93×10^{-4}	1.73×10^{-2}	37.9	16.5
750	4.48×10^{-3}	5.94×10^{-8}	2.88×10^{-6}	1.45×10^{-4}	4.33×10^{-3}	31.9	14.9
1000	8.45×10^{-4}	5.34×10^{-9}	2.88×10^{-6}	2.79×10^{-5}	8.14×10^{-4}	24.7	14.8

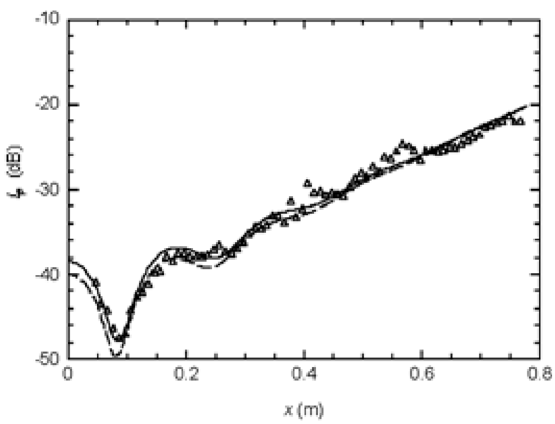

Fig. 4 : Predicted and measured axial sound pressure level in fabric tube at 1 kHz: ———, predicted with radiation load; — — —, predicted without radiation load; Δ, measured data. Dimensionless wall impedance = 9 + i0.5.

The TL figures in Table 1 are impressive. The TL increases as the frequency falls, reaching 41.6 dB at 250 Hz. The radiation loss also increases as the frequency falls, reaching 17.3 dB at 250 Hz. Although data are not available below this frequency, it is likely that even higher TL and Δ_{rad} figures are attainable at lower frequencies. The radiation leakage value at 250 Hz is quite high, and it is observed from Table 1 that over 98% of the incident sound power is dissipated in the walls. As the frequency falls, the tube would be expected to radiate sound progressively less effectively, but the radiation load is sufficiently small to allow significant normal particle motion in the wall, and hence substantial acoustic dissipation. There is likely to be an optimum value for the steady flow resistance of the tube walls. If this is too small, the tube will be too transparent to sound and – while the TL may be high – this will result in Δ_{rad} figures that are too low. Conversely, if the wall flow resistance is too high, then the walls will not allow sufficient radial particle motion to permit strong acoustic dissipation.

Lined ducts with elastic walls

In Figure 5 is shown a rectangular duct with elastic walls, lined internally with a bulk porous sound-absorbing material on all four sides. It contains a uniform mean air-flow, of Mach number M. Sound propagates internally within the duct, both in the "airway" or central flow passage and in the lining. The duct walls respond to the internal sound pressure fluctuations and carry structural waves.One may represent the internal sound field as a summation of coupled structural/acoustic modes, each satisfying the appropriate acoustic and structural boundary conditions: (i) continuity of sound pressure across the interface between the airway and the acoustic absorbent, (ii) continuity of normal particle displacement across this interface, (iii) equality of normal particle displacement in the absorbent and structural displacement of the walls at the internal perimeter of the walls, (iv) appropriate structural boundary conditions at the duct corners, usually continuity of bending moment about the corner, continuity of transverse wall slope (i.e. the duct corners remain right-angled as they rotate), and zero normal wall displacement at the corners. In these coupled modes, the structural and acoustic fields both have the same axial wavenumber. The structural/acoustic mode shapes and axial wavenumbers may be found by a variety of means, but numerical techniques such as the finite element (FE) method are the

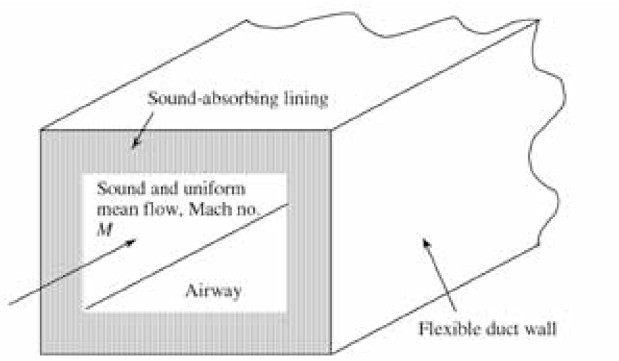

Fig. 5 : Flexible-walled rectangular duct lined internally on four sides, with uniform mean flow

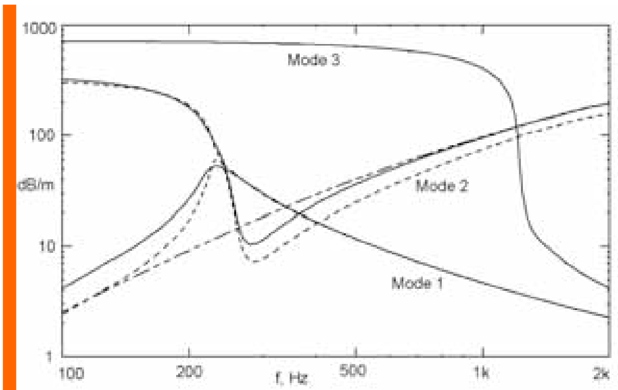

Fig. 6 : Finite element predictions for the axial attenuation rate of coupled structural/acoustic modes in a square section galvanised steel duct with 0.54mm thick walls, lined internally on all four sides with 27mm thick Lancaster Glass Fibre "E glass". ——, M = 0; - - - - , M = 0.1; — - - —, rigid wall mode, M = 0.

most general.
In Figure 6 are shown FE computed data of axial attenuation rate for the lowest three coupled modes (taken from [3]) in the case of a 0.54mm thick galvanised steel duct having a 107mm square cross-section and a 27mm lining of "E glass" (manufactured by Lancaster Glass Fibre) on all four walls. The effects of mean air-flow are included here, and curves are plotted both for zero mean flow speed and for a mean flow Mach number, in the airway, of 0.1. The axial attenuation rate of the fundamental acoustic mode for zero mean flow speed in a rigid-walled lined duct is also plotted for comparison.

The main features of interest here occur in the frequency range 220-230 Hz, and involve "cut-on" for the first structural mode in the duct walls. (Note here that modal cut-on is not such an abrupt phenomenon as it is in the case of unlined ducts, but is measured instead in terms of relative attenuation rate.) Below this frequency, only "mode 1" can propagate with relatively little attenuation; both modes 2 and 3 are highly attenuated. Mode 1 here is a predominantly "acoustic" type mode, with most of the power flow travelling acoustically in the airway and the liner. In the cut-on frequency region, mode 1 displays a dramatic attenuation peak, before becoming an essentially "structural" type mode, with most of its power flow occurring in the walls, and displaying a decreasing attenuation as the frequency rises. Above cut-on, mode 2 becomes a propagating "acoustic" type mode, and – while it has a similar attenuation rate to mode 1 in the cut-on region – it shows an increasing attenuation as the frequency increases, roughly following the trend of the rigid-wall duct mode. Above 350 Hz, mode 1 is less highly attenuated than mode 2 (the difference rapidly increasing as the frequency rises), and is therefore capable of acting as a flanking mechanism if excited to any significant extent. Mode 3 is strongly cut-off below about 1.3 kHz, when its attenuation rate falls rapidly as it approaches cut-on. Two main physical effects are exhibited in Figure 6.

The first of these is the considerable increase in the modal attenuation rate – about six-fold – in both modes 1 and 2 around the first cut-on frequency. This is an effect that can be exploited by the careful design of silencer systems so as to give very high attenuation in fairly narrow frequency bands. The second effect is the role of "structural" type modes in flanking energy paths, where they are lightly attenuated. It is the former effect which is of particular interest here.
Mean flow effects on modes 1 and 2 are broadly as one would expect (see the comments in [3]). Mode 1 exhibits the usual decrease in attenuation in the presence of mean flow in the direction of sound propagation at low frequencies, though when the mode undergoes its transition to "structural" behaviour, flow ceases to have any significant effect. Where mode 2 is cut-off, flow has little effect on its attenuation, but when it becomes an acoustic type mode above about 280 Hz, the flow effects are similar to those on mode 1 below 220 Hz. Mode 3, being essentially cut-off below 2 kHz, shows no mean flow effects on its attenuation.

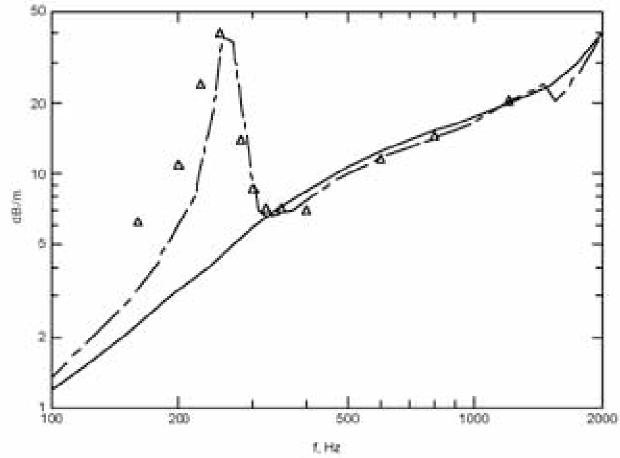

Fig. 7 : Effective axial attenuation rate in a 90mmx100mm duct having three rigid walls and one 100mm flexible wall, of 0.54mm thick aluminium plate. Absorbent is 30mm polyurethane foam, steady flow resistivity 6230 mks rayl/m, placed against the flexible wall. ———, FE predicted, rigid-walled duct; — - —, FE predicted, flexible-walled duct; Δ, measured data

In Figure 7 are shown predicted and experimental data (taken from [2]) for sound propagation in an experimental duct of 90mm¥100mm cross-section, having three rigid walls (of Perspex) and one 100mm flexible wall, of 0.54mm thick aluminium. A 30mm layer of polyurethane foam, of steady flow resistivity 6230 mks rayl/m, was placed inside the duct immediately adjacent to the flexible wall, which was rigidly clamped at the edges. A section of this duct is

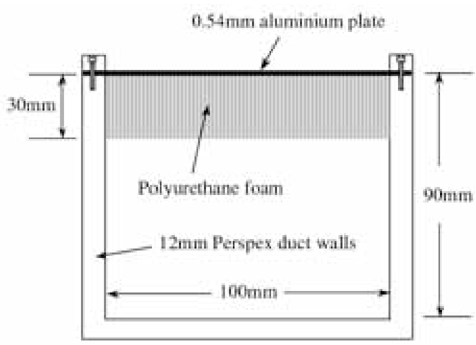

Fig. 8 : Cross-section of the experimental duct.

illustrated in Figure 8.
In the test duct, the fundamental mode acoustic wave, propagating in a lined 90mm¥100mm duct with four rigid walls, was incident upon the flexible-walled section. A series of coupled structural/acoustic modes was generated at the rigid/flexible transition in the duct wall. This somewhat complicated the notion of a constant attenuation rate in dB/m, which – though applicable to individual coupled modes – does not adequately describe the situation in which several modes, having differing attenuation rates, may be present. The "effective axial attenuation rate" was defined as the difference between the sound pressure level at a particular point in one of the rigid duct walls at the rigid/flexible transition, and the sound level at the corresponding point 1m farther from the sound source.

A FE method was used to compute the effective axial attenuation rate, and this included multiple coupled modes. For comparison, the FE computed attenuation rate for the fundamental mode in the equivalent rigid-walled duct is also plotted. Measured data were taken in the experimental duct by means of a probe microphone. The main feature to be noted in Figure 7 is the very striking peak in attenuation rate at 260 Hz. Here, the attenuation rate in the flexible-walled duct is about ten times that in the rigid-walled lined duct. Prediction and measurement agree quite well, given that the anechoic termination in the experimental duct did not work perfectly well at the lower frequencies and would affect the measured data to some extent.
The physical mechanism underlying the attenuation peak has been outlined qualitatively as a "gas-pumping" effect (associated with the fundamental transverse structural resonance in the duct walls) in section 1, and discussed above in terms of combinations of coupled modes in the context of the data in Figure 6. It should be noted that it is only at the fundamental transverse structural resonant frequency of the duct walls that any worthwhile increase in attenuation occurs. Higher structural resonances do not exhibit the same effect. Of course, there is likely to be a certain increase in noise "breakout" from the duct walls associated with increased structural motion at the resonant peak, but this would not necessarily present a problem in practice.

Discussion and conclusions

Two apparently rather unrelated noise attenuation mechanisms have been discussed in this paper. They manifest themselves in rather different practical applications: vehicle inlet systems and sheet metal air ducts. They do, however, have one common feature, which is that the acoustic particle velocity in the sound absorbing material is greater that it is in the situation where the absorbent is contained within rigid duct walls. In the case of porous tubes, the outer impervious covering is not present and so the radial constraint presented by the rigid walls is absent. In the case of ducts with elastic walls, it is the increased wall motion in the neighbourhood of a structural duct wall resonance that brings about the greater particle velocity in the absorbent. In both cases, there is an enhancement of acoustic power loss.
Comparison between these two mechanisms highlights an essential difference between them. In the case of porous tubes the sound attenuation is broadband, without any very dramatic frequency dependence (though with a significant increase as the frequency falls), while in the case of lined ducts with flexible walls, structural resonance effects bring about high attenuation in a fairly narrow frequency band. Since both porous tubes (which are often termed "flexible tubes", though this characteristic appears to play little part in the noise attenuation process) are widely used in automotive applications and lined sheet metal ducting is almost universally employed in air-moving duct silencers, it is clearly of benefit for their noise attenuation characteristics to be optimised. This is possible by the use of predictive software such as that described here.

References

[1] A. CUMMINGS and R. KIRBY 1999 Journal of Sound and Vibration 226, 237-251. Low frequency sound transmission in ducts with permeable walls.

[2] R. J. ASTLEY, A. CUMMINGS and N. SORMAZ 1991 Journal of Sound and Vibration 150, 119-138. A finite element scheme for acoustical propagation in flexible walled ducts with bulk reacting liners, and comparison with experiment.

[3] R. KIRBY and A. CUMMINGS 1998 Proceedings of ISMA23, Leuven, Belgium, 677-684. Structural/acoustic interaction in air-conditioning ducts in the presence of mean flow.

[4] A. CUMMINGS, H. J. RICE and R. WILSON 1999 Journal of Sound and Vibration 221, 143-167. Radiation damping in plates, induced by porous media.

■